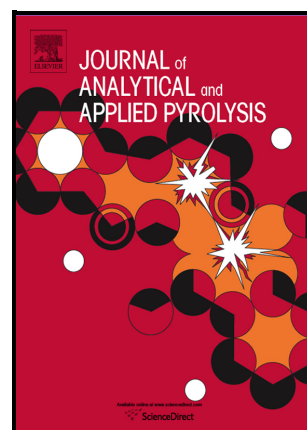


Journal Pre-proof

Analytical fast pyrolysis of *P. Juliflora*: A thermal and catalytic study

Mpho Thabang Rapoo, Saranpreet Singh, Katie Chong, Scott Banks, Paula H. Blanco Sanchez



PII: S0165-2370(23)00398-4

DOI: <https://doi.org/10.1016/j.jaap.2023.106254>

Reference: JAAP106254

To appear in: *Journal of Analytical and Applied Pyrolysis*

Received date: 22 August 2023

Revised date: 24 October 2023

Accepted date: 6 November 2023

Please cite this article as: Mpho Thabang Rapoo, Saranpreet Singh, Katie Chong, Scott Banks and Paula H. Blanco Sanchez, Analytical fast pyrolysis of *P. Juliflora*: A thermal and catalytic study, *Journal of Analytical and Applied Pyrolysis*, (2023) doi:<https://doi.org/10.1016/j.jaap.2023.106254>

This is a PDF file of an article that has undergone enhancements after acceptance, such as the addition of a cover page and metadata, and formatting for readability, but it is not yet the definitive version of record. This version will undergo additional copyediting, typesetting and review before it is published in its final form, but we are providing this version to give early visibility of the article. Please note that, during the production process, errors may be discovered which could affect the content, and all legal disclaimers that apply to the journal pertain.

© 2023 Published by Elsevier.

Analytical fast pyrolysis of *P. Juliflora*: A thermal and catalytic study

Mpho Thabang Rapoo^a, Saranpreet Singh^a, Katie Chong^a, Scott Banks^a, Paula H. Blanco

Sanchez^{a*}

Energy & Bioproducts Research Institute (EBRI), Aston University, B4 7ET. Birmingham, UK.

*Corresponding author email address: p.blanco-sanchez@aston.ac.uk

1. Abstract

Thermal and catalytic fast pyrolysis of *Prosopis juliflora* (*P. juliflora*), fractions namely wood, seed pods, leaves and their mixtures (wood: seeds: leaves at 80:10:10, and seeds: leaves at 50:50) were investigated. Fast pyrolysis tests were performed in a py-GC/MS to study the product distribution at 450, 500 and 550 °C. Further catalytic tests at 500 °C, used HZSM-5, 1wt.% Ni-HZSM-5 and 5wt.% Ni-HZSM-5, and the wood fraction as feedstock. For all the non-catalytic thermal tests, significant proportions of acids, ketones, aldehydes, sugars, alcohols, phenols, nitrogenous compounds (NITs) and other oxygenates were observed. Out of the three *Prosopis* fractions studied, the wood at 500 °C yielded the highest amount of ketones, aldehydes and phenolics (78.67%), whilst the mixture (wood: seeds: leaves at 80:10:10), yielded 83.04%. This suggests that *Prosopis* feedstock can be processed as a mixture thus eliminating the need for pre-separation. The catalytic tests were completed at 500 °C with catalyst: biomass ratios (C/B) of 3:1, 6:1 and 9:1. The use of zeolite-based catalysts, improved the product distribution by forming aromatic hydrocarbons (monocyclic) and polycyclic aromatic hydrocarbons (PAHs) thus reducing the proportion of oxygenates detected in the thermal tests. The addition of nickel to the zeolite catalyst (9:1 C/B ratio; 5 wt.% Ni-HZSM-5), resulted in aromatics and polyaromatic hydrocarbons (PAHs) yields of 60.28% and 27.50%, respectively. Overall, the tests using Ni-loaded zeolites showed selectivity towards aromatics, as higher proportions were obtained when compared to PAHs. Our results correlated the

influence of specific components in the individual fractions of *Prosopis* (wood, seeds, and leaves) on the pyrolysis products. We established the potential of using an invasive plant to yield aromatics, which are main components for biofuels production, thus proposing a sustainable pathway to manage its spread and to yield a high-value product.

Key words: *P. juliflora*, catalytic fast pyrolysis, py-GC/MS, zeolite, HZSM-5, aromatics

2. Introduction

Prosopis (*Mesquite*) is a leguminous plant of over 40 different species [1]. It is native to tropical America and has been adopted and introduced to countries with arid regions to improve fodder resources and combat desertification [1]. Such countries include Botswana, South Africa, Namibia and India. However, *Prosopis* plants tend to proliferate and become a threat to plant biodiversity [2]. As a result, *Prosopis* species are considered invasive in these countries and a species of concern in other territories such as the UK [3-5]. As these plants are available abundantly and grow at a considerable rate, with a growth rate of 25 km²/ year reported [6], they could be utilized as a biomass resource for biofuel production which would provide a way of managing their spread or removal [3]. *Prosopis juliflora* (*P. juliflora*) is the most common *Prosopis* species and will be explored in the present study as a biomass resource for high value products via pyrolysis [2].

Pyrolysis is a thermochemical conversion process which entails heating a material in an oxygen deprived environment. The pyrolysis products are a liquid (bio-oil) consisting of acids, sugars and oxygenated hydrocarbons (aldehydes, alcohols, ketones, esters, ethers, phenols, moisture), a solid fraction (char), and a gas fraction (pyrolysis gas) [7-9]. The properties of crude bio-oil inhibit its use as an alternative to petroleum fuel due to high acidity, high oxygen, and moisture content, high viscosity, and low heating value [10, 11].

Bio-oil can be upgraded to more stable hydrocarbons using catalysts. Different catalysts have been studied for bio-oil upgrading, however zeolite-based catalysts have been widely

researched in catalytic cracking of bio-oil as they have shown better performance in terms of facilitating the target reactions such as dehydration, decarboxylation, decarbonylation and aromatisation compared to other catalysts [12, 13]. Zeolites have high selectivity towards hydrocarbon production and can limit unwanted products like oxygenated compounds and carboxylic acids [12, 14, 15].

Zeolite Socony Mobil-5 (ZSM-5) has been researched as a potential candidate for upgrading fast pyrolysis vapours in catalytic fast pyrolysis due to its impressive shape selectivity and excellent deoxygenating capability [12]. Thangalazhy-Gopakumar et al. [16] reported an increase in aromatic hydrocarbons with increased catalyst load from pyrolysis of algal biomass using ZSM-5. The highest content was 50.8 wt.% of aromatic hydrocarbon from a catalyst: biomass (C/B) ratio of 9:1 at a temperature of 650°C in a pyroprobe was obtained due to the increased number of active sites in the catalyst.

Another zeolite which has commonly been explored is HZSM-5, the protonated version of ZSM-5. When used, it significantly reduced the oxygen content in the bio-oil [14]. HZSM-5 is reported to have better thermal and hydrothermal stability as well as better shape selectivity and stronger acidity compared to ZSM-5, thus it is more effective at producing aromatics than the latter [14]. It is reported to successfully reduce oxygen content, increase the higher heating value, and reduce bio-oil acidity [8, 17, 18]. HZSM-5 has a unique pore structure which results in its heightened selectivity of aromatics; showing better selectivity to monocyclic aromatics which promotes the yield of aromatics in the process [19]. In the pyrolysis of pine over HZSM-5 in bench scale a fluidised bed reactor for in-situ and ex-situ upgradation, Iisa et al. [19] found that the upgraded bio-oil was ~45 wt. % lower in oxygen content than non-upgraded oils. They reported similar reduced oxygen and water contents in the oil, similar oil yields of 14 – 17 wt. % but more catalyst deactivation due to coke formation in the in-situ reactor set up than ex-situ [19].

Zeolites can be modified to improve their performance in upgrading bio-oil. Studies have reported that metal loaded zeolite catalysts demonstrate enhanced acidity, reduced oxygenate production as well as a higher resistance to the formation of coke [20-23]. Nickel loaded H-ZSM-5 has particularly shown selectivity towards aromatics for fuel [20, 22]. French and Czernik [24] in their study of catalytic pyrolysis of Aspen wood at 600 °C with metal loaded ZSM-5 observed the highest yield of upgraded bio-oil, containing hydrocarbons when using Ni as the metal compared with other metals which included Ga, Co, Fe, Ce, Cu and Na. They attributed this to the high catalytic activity coupled with higher reaction temperature leading to more volatiles. Yung et al. [20] found that adding Ni improved the performance of ZSM-5 in that it exhibits strong hydrogenation activity which enables it to hydrogenate some of the compounds to convert them to hydrocarbons. They reported that the addition of Ni to the surface and pores of the support prevents the pores to be clogged by coke through enhanced hydrogenation reactions, their tests were performed on southern pine [20]. Veses et al. [21], reported a reduction in phenolics with the use of Ni-ZSM-5 in the upgrading of bio-oil from pyrolysis of woody biomass. The highest production of hydrocarbons in comparison to other metals like Cu, Mg, Sn and Ga was observed with the use of Ni, however Ga also displayed a comparable reduction of phenolics to Ni [21].

Pyrolysis-gas chromatography and mass spectroscopy (py-GC/MS) is a technique adopted to study the behaviour of biomass under different experimental conditions as well as the influence of these conditions on the product distribution obtained in the pyrolysis volatiles while providing simplicity in operation [25, 26]. It gives insight into the proportion of compounds contained in the pyrolytic volatiles and is reported to detect compounds which form the condensable (liquid) fraction more efficiently than in GCMS of the fraction which would require full condensation prior to analysis [26]. Work using py-GC/MS in studying the

performance of zeolites such as HZSM-5 in catalytic biomass pyrolysis has reported that these catalysts can effectively convert oxygenated hydrocarbons into aromatics [27].

In the present work, the thermal pyrolysis of three of the fractions of the *P. juliflora* plant (wood, seed pods and leaves) and their mixtures (wood, seeds and leaves: WOSDLV; seeds and leaves: SDLV), was performed in a py-GC/MS at three temperatures 450, 500 and 550 °C. To the best of the authors' knowledge, there has been no work on thermal and catalytic pyrolysis of these three fractions of *P. juliflora* as well as their mixtures, especially using py-GC/MS. The catalytic tests were carried on the wood sample (main plant component), at 500 °C, and at three catalyst: biomass (C/B) ratios (3:1, 6:1, 9:1). The catalysts used were HZSM-5 and two nickel loaded HZSM-5 catalysts (1wt.% and 5 wt.% nickel loadings). Details on the characterisation techniques used for samples, products, and catalysts, can be found in the methods section. This work will contribute to work that promotes the utilisation of this invasive plant as a means of managing their spread.

3. Materials and methods

3.1 Biomass samples

The three fractions of the *P. juliflora* tree, leaves, seed pods and wood, were collected from the Kgalagadi district, Botswana on 9th January 2022. The latitude and longitude of the site are 24.89156° S, 23.23316° E. The tree was selected according to the field guide of identifying *Prosopis* species by Pasiiecznik et al. [1], which suggests to undertake a comparison of the seed pods, leaves and tree structure (height, branches, whether it has a trunk or not) to distinguish it from other *Prosopis* species like *Acacia*, and *Mimosa*. The selected tree, satisfied the described characteristics of *P. juliflora* as per Table 1 [1]. The reported guide was also used to differentiate and collect the leaves, seed pods and wood fractions. Each of the fractions were manually separated with a panel hacksaw, then air-dried at room temperature for 24 h, and finally placed in a drying oven at 60 °C for 24 h to reduce excess moisture. They were then

grinded using an IKA WERK M20 grinder, following a sieve shaker to obtain a particle size distribution of 106 – 250 μm (analytical fraction). The mixtures of the individual samples were prepared by measuring out quantities of the components to obtain desired proportions of 80:10:10 for wood, seed pods, and leaves (WOSDLV); and 50:50 for seed pods, and leaves (SDLV). These proportions were adopted as they were representative of the quantities of fractions on the plant.

Table 1: Characteristics of *P. juliflora* [1].

Height (m)	Trunk	Branches	Thorn type & length (cm)	Foliage	Flower/ raceme length (cm)
3 – 12	–	Spreading/ shrubby	Solitary/ paired (0.5 – 5)	Glabrous/ pubescent	7 – 5

3.2 Catalyst preparation

HZSM-5 was obtained in ammonium form (NH_4^+) from Alfar Aesar by Thermo Fischer Scientific (Si/Al ratio = 30). It was transformed to protonic form (H^+) by calcining in a muffle furnace at 600 $^\circ\text{C}$ for 6 h with a ramp rate of 10 $^\circ\text{C}/\text{min}$. Modified Nickel/HZSM-5 (Ni-HZSM-5) at 1wt.% and 5 wt.% loading was prepared by incipient wetness impregnation method. Appropriate amounts of $\text{Ni}(\text{NO}_3)_2 \cdot 6\text{H}_2\text{O}$ (99.999% Sigma Aldrich, UK) were dissolved in de-ionised water at room temperature to prepare aqueous precursor solutions of nickel (II) nitrate hexahydrate to obtain the 1wt.% and 5wt.% Ni loadings. The precursor solutions were introduced to the protonated ZSM-5 catalyst, the mixture was stirred with a magnetic stirrer at room temperature for 4 h, following which it was left to air dry for 15 h. The slurry was then placed in a drying oven at 110 $^\circ\text{C}$ for 5 h, then calcined at 550 $^\circ\text{C}$ in air atmosphere under static conditions for 5 h in a muffle furnace (ramp rate of 5 $^\circ\text{C}/\text{min}$), to decompose the nickel nitrate and obtain nickel oxide. The resulting catalysts were crushed in a ceramic mortar and pestle

and sieved to obtain a particle fraction of 106 – 250 μm , to ensure uniformity with the biomass *P. juliflora* sample particle size. The final catalysts were assigned as 1wt.% Ni-HZSM-5 and 5wt.% Ni-HZSM-5.

3.3 Catalyst characterisation

X-ray diffraction (XRD) was performed to study the crystalline structure of the catalyst, this was completed using an X-ray Diffractometer (Malvern Panalytical Empyrean, Netherlands) with Cu K α radiation ($\lambda=1.5418\text{\AA}$) operating at 40 mA and 40 kV, scanning from 5 to 80° 2 θ every 0.02° (2 θ) with counting time 2s per step. The Nova 4000 porosimeter equipped with an Automatic Volumetric Sorption Analyzer, used the Brunauer–Emmett–Teller (BET) and the Barrett, Joyner, and Halenda (BJH) methods at -196 °C with liquid nitrogen, to determine the surface area (S_{BET}), pore volume and mesopore size distribution of the catalysts. The samples were degassed for 5 h at 120 °C under 5×10^{-9} Torr vacuum. The pore size distribution was obtained by applying the BJH modified by Kruk, Jaroniec and Sayari (BJH–KJS) model to the adsorption branch of the isotherm. The T-plot method was used to discriminate between micro- and meso/microporosity. The meso/macropore volume was determined by subtracting the micropore volume (from T-plot analysis) from the total pore volume (at $P/P_0 = 0.99$). This analysis was carried out in duplicate.

3.4 *P. juliflora* characterisation

Elemental analysis of the ground sample was performed on a CHNS-O Flash 2000 Organic elemental analyser from Thermo-Scientific on a sample of ca. 3mg mass. The operating conditions were 900 °C for the furnace temperature, and 50 °C for the oven; the carrier gas was high purity oxygen at 3.5 bar and 140 mL/min flowrate. A thermal conductivity detector (TCD) with a filament was used with $\sim 1000 \mu\text{V}$ intensity. The calibration was undertaken using standard sulphamide and vanadium pentoxide as oxidising agent. The analyses were carried out in triplicate. The proximate analysis was performed on a thermogravimetric analyser

(TGA/DSC 2 STAR system, Mettler Toledo, with alumina 70 μl crucible) in N_2 and O_2 atmospheres on a sample size of ca. 3mg. The temperature increased from 25 to 900 $^\circ\text{C}$ at 10 $^\circ\text{C}/\text{min}$ ramp rate under nitrogen atmosphere, followed by isothermal conditions at 900 $^\circ\text{C}$ for 20 minutes under oxygen.

3.5 Py-GC/MS experiments

Analytical pyrolysis (thermal and catalytic) of the *P. juliflora* samples (wood, leaves, seed pods, WOSDLV and SDLV), was carried out in a Single-shot Pyrolyser PY-3030S (Frontier lab) close-coupled to a Shimadzu QP2010E Gas Chromatograph Mass Spectrometer (GC-MS) (Shimadzu Corporation, Kyoto, Japan). All pyrolysis experiments used 0.5 mg of *P. juliflora* sample weighed into stainless-steel crucibles (Frontier lab, Eco-cup LF). The thermal experiments were performed at temperatures of 450, 500, 550 $^\circ\text{C}$ for each sample. The catalytic experiments were performed at 500 $^\circ\text{C}$, using three catalyst to biomass (C/B) ratios of 3:1, 6:1 and 9:1. Appropriate amounts of biomass and catalyst were weighed in the crucibles and mixed uniformly using the Eco-stick SF, to finally ensure the desired C/B ratios were achieved.

All the pyrolysis experiments (thermal and catalytic) were performed at 20 $^\circ\text{C}/\text{ms}$ heating rate, 15 s hold time under He carrier gas flow at 1.91 mL/min. The components were separated using a Perkin Elmer Elite-1701 column (cross-bond: 14% cyanopropylphenyl and 85% dimethyl polysiloxane; 30 m, 0.25 mm inner diameter, 0.25 μm film thickness). The GC oven was held at 45 $^\circ\text{C}$ for 1 minute, then heated at 5 $^\circ\text{C}/\text{min}$ to 275 $^\circ\text{C}$ and held at this temperature for 3 minutes leading to a total time of 50 minutes for the experiment. The separated components were identified in mass spectra of 45-300 m/z every 0.2 secs. The NIST 2011 MS library was used to assign individual peaks in the chromatogram from the pyrolysis vapours with a match factor of 80% and quantification was made using peak areas in the chromatogram. The thermal tests were performed in duplicate at 450 $^\circ\text{C}$ to ensure repeatability. The resulting chromatograms showed high comparability as there was negligible difference between them.

The same was done for catalytic tests at the same C/B ratio (3:1) and the chromatograms for these tests showed consistency.

4. Results and Discussion

4.1 Feedstock characterisation

In this section, the results of the proximate and ultimate analysis of *P. juliflora* fractions (wood, leaves, seed pods) and the fractions mixtures (WOSDLV, SDLV) will be discussed.

4.1.1 Proximate and ultimate analysis

Table 2 shows a comparison between the proximate and ultimate analysis of the *P. juliflora* wood from this work with data from literature. The results from the wood sample (present study) either show a slight variation or close similarity depending on the parameter when compared to those from other studies which tested *P. juliflora* wood. Close similarity is observed in the ultimate analysis data, while variation is noticed in the proximate analysis. For example, the volatile matter of the wood sample, the present study is 79.75% while the highest value from the literature is 69.80% [28]. This variation in data between the current study and that from literature can be attributed to the use of different analytical methods and differences in plant growth due to varied soil compositions at the different locations from which the plants grew [29].

The properties of seed pods (Table 3), and *P. juliflora* leaves, WOSDLV and SDLV and mixtures (Table 4) are assessed and linked to their thermal degradation behaviour. In Table 3, values for seed pods show a significant variation, which can also be due to different analysis methods and plant growth conditions. So far in the literature, it has not been reported details on *P. juliflora* leaves or WOSDLV and SDLV mixtures, therefore no comparison is reported (Table 4) [28, 30, 31]. The volatile matter for wood sample (79.75%, Table 2) is followed by the WOSDLV mixture at 79.12 wt.% (Table 4), which could be due to the influence of the wood fraction in the sample. Fixed carbon content is observed to be highest in the seed pods at

18.80 wt.% (Table 3) and is least in the leaves at 10.44 wt.% (Table 4). The carbon content ranges between 43.50 wt.% and 45.83wt.% for all the samples (Tables 2-4). Both the fixed carbon and the carbon content have been reported to be directly proportional to the higher heating value [29, 30]; whereas the oxygen content in all samples is high which would potentially reduce their heating values [30]. The leaves have the highest ash content (6.70 wt.%) suggesting it would have the lowest energy content whilst the lowest ash content is observed in the wood at 2.08 wt.%.

Low nitrogen and sulphur content deem *P. juliflora* a more environmentally benign energy source compared to fossils as it will produce low SO_x and NO_x during conversion. The highest nitrogen and sulphur content is found in the leaves which is consistent with them containing chlorophyll. The mixed samples show values comparable with the individual fractions indicating a clear influence of individual fractions properties on the studied mixtures.

4.1.2 Thermogravimetric analysis

To assess the pyrolysis behaviour of *P. juliflora* individual fractions and mixtures, a thermogravimetric analysis (TGA) was performed. The TGA and DTG curves are shown in Figures 1(a) to (e). Figure 1(a), (c) and (d) show that degradation occurs in three stages which agrees with what has been reported in other work [6, 30]. However, Figures 1(b) and (e) for seed pods and SDLV mixture, show more than three stages of decomposition, this can be attributed to individual degradation of seeds and the pods (seed covers), this is more evident in the mixture sample containing seed pods (SDLV, Figure 1e). In Figure 1(a), and (d) it is observed that the first stage (40 – 235 °C) of moisture removal occurs as well as the release of lighter volatiles as hemicellulose starts to degrade. The derivative thermograph (DTG) for this stage shows numerous small peaks as the loss of moisture is an endothermic process [30]. The second stage (235 – 440 °C) is characterised by a rapid decline in thermographs due to the breakdown of hemicellulose from 235 – 305 °C, and cellulose from 305 – 400 °C. The peaks

	4.93 ±	79.75 ±	13.21	2.08 ±	45.57	5.89	47.75	0.79	0.00
Present study	0.04	0.29	± 0.31	0.02	± 0.21	±	± 0.25	±	
						0.06		0.02	
Suriapparao	9.00 –	62.70 –	16.80 –	1.00 –	43.01	6.27	45.99	1.39	0.09
et al. [35]	12.50	67.90	24.80	5.50	–	–	–	–	–
					44.97	7.06	48.67	1.89	0.38
Chandran et	6.70 –	64.50 –		2.40 –					
al. [30]	6.90	65.10	-	2.70	45.60	6.20	47.10	0.90	0.30
					44.68	5.96		1.58	0.06
Chandraseka	7.90 –	68.30 –	17.90 –	2.40 –			42.69		
ran et al. [28]	11.20	69.80	19.10	3.02	–	–	–	–	–
					47.32	8.08	– 47.6	1.83	0.08

^a Dried sample; * Obtained by difference on present study.

Table 3: Proximate analysis (on dry basis) and ultimate analysis of *P. juliflora* seed pods.

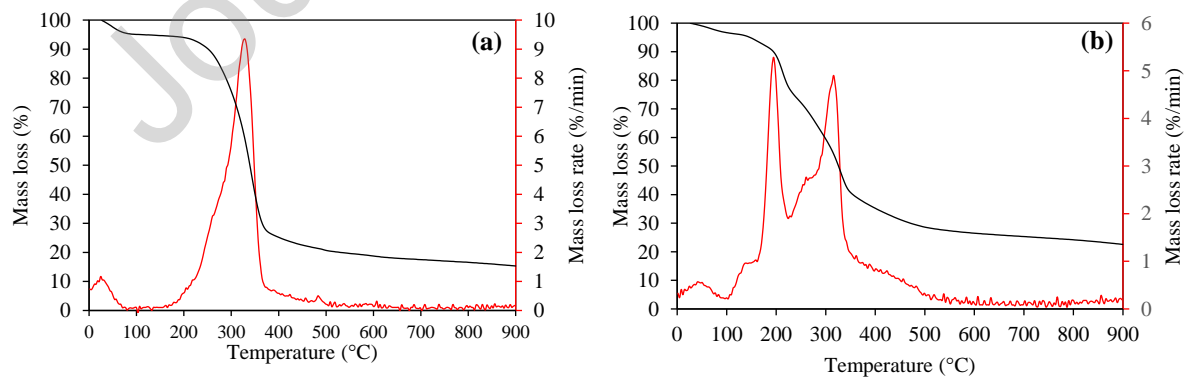
Reference	Proximate Analysis (wt. %)					Ultimate Analysis (wt. %)				
	Sa mp le ^a	Moistur e content	Volatil e matter	Fixed Carbo n	Ash Conte nt	C	H	O*	N	S
Present study	See pod s	3.20 ± 0.18	74.20 ± 0.17	18.80 ± 0.07	3.80 ± 0.22	43.72 ± 0.35	6.18 ± 0.03	48.19 ± 0.27	1.78 ± 0.08	0.13 ± 0.02
Gayathri & Uppuluri [29]	See pod s	7.90 ± 0.002	87.67 ± 0.002	4.23 ± 0.002	0.21 ± 0.002	41.77 0.002	6.55	21.8	3.59	26.3 0

^a Dried sample; * Obtained by difference on present study.

Table 4: Proximate analysis (on dry basis) and ultimate analysis of mixtures of *P. juliflora* leaves, WOSDLV, and SDLV.

Sample ^a	Proximate Analysis (wt. %)				Ultimate Analysis (wt. %)				
	Moisture content	Volatile matter	Fixed Carbon	Ash Content	C	H	O*	N	S
Leaves	4.91 ± 0.01	77.95 ± 0.13	10.44 ± 0.20	6.70 ± 0.25	45.83 ± 0.13	6.22 ± 0.10	43.70 ± 0.19	3.82 ± 0.05	0.42 ± 0.01
WOSDLV (80:10)	5.20 ± 0.07	79.12 ± 0.12	12.58 ± 0.26	3.11 ± 0.11	44.18 ± 0.18	6.05 ± 0.10	48.65 ± 0.13	1.12 ± 0.30	0.00
SDLV (50:50)	3.98 ± 0.10	76.20 ± 0.05	14.69 ± 0.06	5.13 ± 0.09	43.50 ± 0.77	6.38 ± 0.77	47.80 ± 1.16	2.17 ± 0.18	0.15 ± 0.20

^a Dried sample; *Obtained by difference.



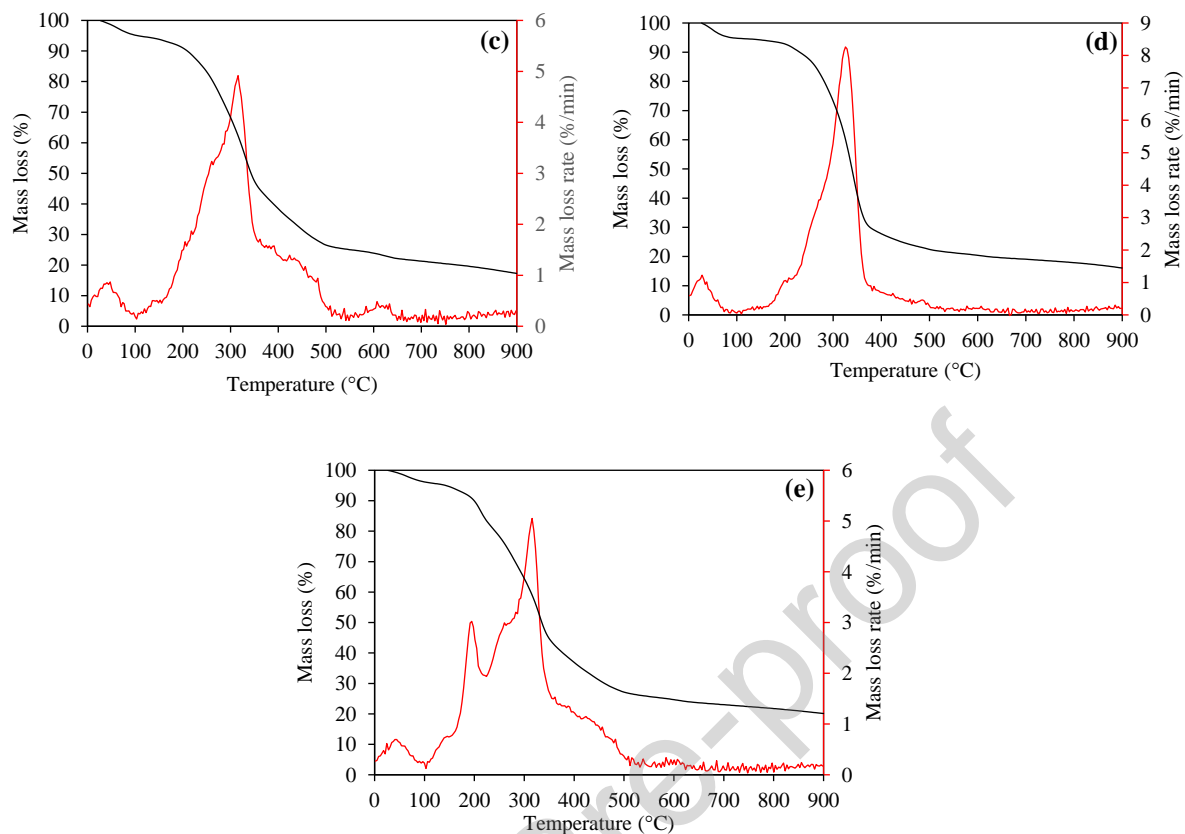


Figure 1: Thermal degradation profiles (TGA and DTG) of *P. juliflora*: (a) wood; (b) seed pods; (c) leaves; (d) WOSDLV (80:10:10); (e) SDLV (50:50).

4.2 Catalyst characterisation

Results from the X-ray diffraction and N_2 porosimetry of HZSM-5, 1wt.% Ni-HZSM-5 and 5wt.%Ni-HZSM-5 catalysts, are presented and discussed below.

4.2.1 X-ray diffraction (XRD)

Figure 3 shows the XRD patterns for HZSM-5, 1wt.% Ni-HZSM-5 and 5wt.% Ni-HZSM-5. The diffraction pattern for all the catalysts are indicative of a Mobil-type 5 (MFI) zeolite structure, which includes peaks between 7° and 9° , and between 23° and 25° [36]. These peaks are well defined in the Ni-loaded catalysts, indicating the crystallinity was maintained even after being subjected to impregnation, calcination and loading of nickel species [36, 37]. It was not possible to distinguish the Ni-loaded characteristic diffraction peaks from the non-loaded ones, suggesting uniform dispersion on the HZSM-5 surface [36, 37]. This is desirable as it

will suggest more accessibility and availability of Ni active sites. However, the triplet of peaks between 23° and 25° linked to ZSM-5 seemed to be reduced when the nickel is added, and further decreased for a higher nickel loading (5wt.%). This reduction might suggest that the metal ions penetrated the pores of the zeolite altering its pore structure [37], or by nickel replacing some of the alumina (Al) in the zeolite framework as suggested by Zhou et al. [38].

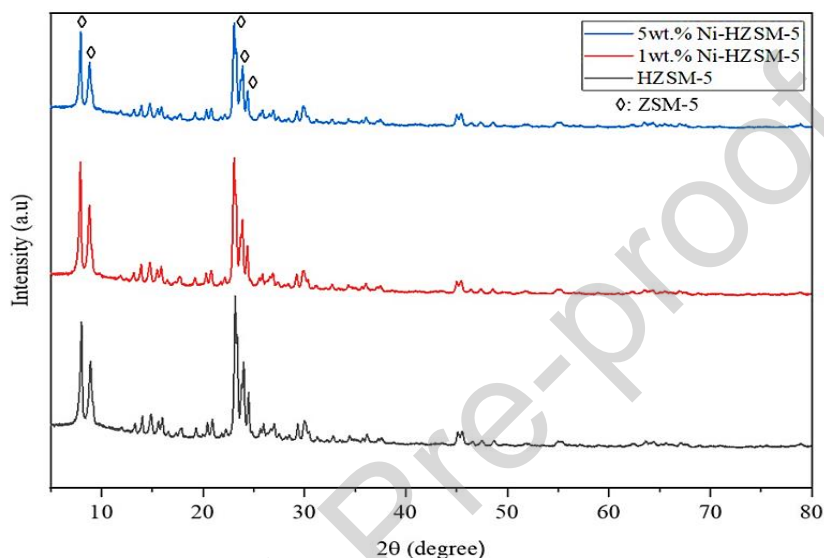


Figure 2: Powder XRD patterns for all samples of fresh zeolite catalysts.

4.2.2 N₂ porosimetry

The physiochemical properties of the fresh zeolite catalysts (HZSM-5, 1wt.% Ni-HZSM-5 and 5wt.% Ni-HZSM-5) are shown in Table 5. Introducing Ni resulted in an increase of the surface area from $410.901 \text{ m}^2/\text{g}$ (HZSM-5) to $440.889 \text{ m}^2/\text{g}$ in 1wt.% Ni-HZSM-5 but it reduced to $380.462 \text{ m}^2/\text{g}$ in 5wt.% Ni-HZSM-5. 1wt.% Ni-HZSM-5 displays the highest surface area, suggesting that the metal species dispersed uniformly on the catalyst surface and may have caused the formation of additional mesopores which resulted in increased surface area [39, 40]. However, increasing the Ni load to 5wt.% caused a reduction in the surface area, which can be attributed to blockage of catalyst pores due to the higher quantity of the metal species [41]. The pore volume appears to increase with the incorporation of Ni, from 0.100 cc/g for HZSM-5, to 0.102 cc/g for 1wt.% Ni-HZSM-5, which is the highest value of the three. This phenomenon

was described by Zhong et al. [42] who attributed this to Ni metal layers being overlaid on each other on the catalyst surface thus enlarging the pore volume. The pore volume then reduces to 0.077 cc/g with higher metal loading of 5wt.% Ni. This agrees with the prior suggestion that the metal species were evenly dispersed on the catalyst surface, however the higher metal loading resulted in pore blockage as the pore volume reduced with 5wt.%Ni. The pore diameter for HZSM-5 was determined as 3.080 nm, and slightly increased when adding nickel to 3.082 and 3.088 nm for 1wt.% and 5wt.% Ni respectively, which indicates the nickel loadings are not blocking the pores accessibility in the catalyst. These values fall within the mesoporous materials range of 2.0 – 50.0 nm [43].

The BET isotherms for all the catalysts (Figure 3) appear to obey type IV of the IUPAC (International Union of Pure and Applied Chemistry) classification, which would be classified as mesoporous materials which is consistent with the pore diameter reported prior. Furthermore, the hysteresis loop is consistent with H4 hysteresis which suggests existence of micropores and mesopores amongst the zeolite particles, this is also supported by the overlap in the absorption and desorption isotherms [40, 44]. This indicates that the initial structure of the micropores and mesopores was maintained even following the addition of Ni [45]. The pore distribution demonstrated by the three catalysts are favourable of formation of aromatics from pyrolysis products. Addition of Ni enhances the pore distribution by formation of mesoporous structure which would enhance the effectiveness of the catalyst in the production of aromatics, hence a higher proportion of aromatics is expected in the Ni modified zeolites [37].

Table 5: Physiochemical properties of fresh zeolite catalysts

Catalyst	S_{BET} (m²/g)	Pore volume (cc/g)	Pore diameter (nm)
HZSM-5	410.901 ± 18.366	0.100 ± 0.025	3.080 ± 0.006
1wt.%Ni-HZSM-5	440.889 ± 51.516	0.102 ± 0.010	3.082 ± 0.008
5wt.%Ni-HZSM-5	380.462 ± 26.285	0.077 ± 0.001	3.088 ± 0.015

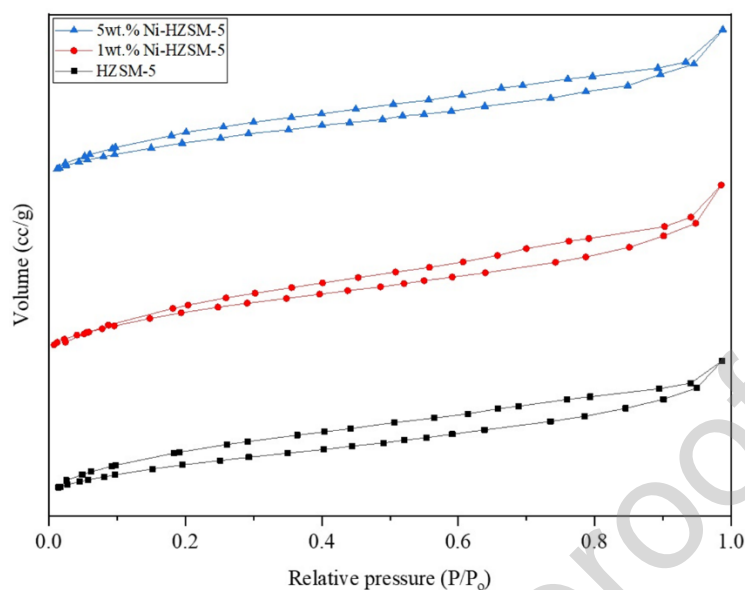


Figure 3: N₂ physisorption isotherms of fresh zeolite catalysts

4.3 Py-GC/MS analysis

Results on thermal pyrolysis of *P. juliflora* fractions (wood, leaves, seed pods) and mixtures of the fractions (WOSDLV, SDLV) at 450, 500 and 550 °C, and catalytic pyrolysis of wood fraction at 500 °C will be discussed in this section.

4.3.1 Thermal pyrolysis

The pyrolysis of *P. juliflora* (wood, seed pods, leaves and mixtures: WOSDLV and SDLV) were carried out in a py-GC/MS at three different temperatures 450, 500 and 550 °C. The temperature influence on products distribution was studied. Chromatograms from the pyrolysis of *P. juliflora* wood, seed pods, leaves (WOSDLV) (80:10:10) mixture at 500 °C is available in the supplementary material (Figure S1). Following identification of compounds in the pyrolysis products through NIST library, compounds were grouped into major compound classes as shown in Table 6. Furthermore, some compound classes were grouped into one major class named ‘compounds of interest (COI)’ for the purpose of this study which is interested in compounds that lead to higher yields of aromatics for the application of transportation fuel. These compounds include oxygenated aromatics, ketones, aldehydes, ethers, alcohols, esters,

acids, and phenols. Figure 4 - 8 show the proportions of functional groups from the thermal pyrolysis of *P. juliflora*. There is a slight variation observed in the product distribution of pyrolysis vapours at the three temperatures across all the samples. This could be because the difference in the temperatures was not substantial enough to cause a notable change in the product distribution as was reported by Arabiourrutia et al. [46] who observed a moderate change in product distribution for thermal pyrolysis of date palm seeds in a pyGC/MS at 450 and 500 °C. However, although the change is moderate, some trends can be observed regarding the products identified at these conditions. This is expected as temperature has been found to be an important parameter in influencing the products obtained from biomass pyrolysis, which has also been observed in some work involving biomass testing in py-GC/MS [25, 26, 46, 47]. It is observed that the compound class with highest proportion in the wood sample across all temperatures was oxygenated aromatics (OxyAR). There was a slight increase in the OxyAR proportions with the rise in temperature, from 28.69% at 450 °C to almost equal proportions at 500 and 550 °C, of 33.46% and 33.25% respectively. The prevailing compounds in OxyAR are a variety of phenol derivatives such as 2,6-dimethoxy-phenol which would be products evolving from lignin decomposition [48]. The higher proportion of this compound group at higher temperatures is due to the enhanced fragmentation and depolymerization reactions experienced by the biomass building blocks, cellulose, hemicellulose, and lignin at higher pyrolysis temperatures [49, 50]. The proportion of phenols was similar in the wood at all temperatures with the highest quantity of 5.12% observed at 500 °C. Products which evolve mostly from cellulose and hemicellulose including ketones, acids, and aldehydes, anhydrosugars, alcohols, ethers, and esters were identified as well, with the first four mentioned having more significant quantities compared to the others. The quantity of aldehydes like furfurals and sugars such as levoglucosan slightly decreased with increased temperature, while ketones increased as was also observed by Bensidhom et al. [26]. Aliphatics (alkanes and

alkenes) and aromatics were detected in little to no proportions in wood as seen in Figure 4. Aromatics were detected only at 550 °C (0.42%) and aliphatics were found to be highest at 500 °C at 1.77% while no polycyclic aromatic hydrocarbons (PAHs) were found, indicating the need for upgrading of pyrolysis vapours.

Acids that were identified included methoxyacetic acid, formic acid and propanoic acid, with the former being the most abundant in the acids group. A notable decline in the proportion of acids with higher temperature was observed with 16.99% observed at 450 °C and 10.50 % and 13.63% at 500 and 550 °C, respectively. This can be attributed to the higher temperatures having an influence on the decomposition reactions of cellulose and hemicellulose as was the case in Bensidhom et al. [26] who used date palm waste as the biomass, and Xin et al. [25] where pine wood was the feedstock. As mentioned before, in this study, all these compounds will be considered as COI for the potential synthesis of aromatics. When the products are considered in this manner, the highest quantity of 78.67% is observed at 500°C, however there is only a small difference compared to the other temperatures which were 76.42% at 450 °C and 76.44% at 550 °C.

Nitrogenous compounds (NITs) were produced in all samples; however, less were detected in wood compared to the seed pods and leaves. These NITs include amides, nitriles, and N-containing heterocycles which have been found in bio-oil from other biomass especially those deemed to be protein-rich [51-53]. *Prosopis* is described to be a nitrogen fixing plant, which can be linked to the proportion of NITs found in its pyrolysis vapours [54]. The quantities of NITs increase with elevated temperature, implying that higher temperature promotes their production which is reported to be through the decarboxylation and cracking of amino acids to form amines, amides and nitriles, as well as dehydrogenation, dehydration and cyclisation of the latter compounds to form their derivatives [51, 55, 56].

The highest proportion of COI in the seed pods at 82.51% was observed at 450 °C, followed by 77.48% and 75.72% at 500 and 550 °C respectively (Figure 5). This is unexpected as the opposite should have occurred due to molecule degradation at higher temperature. A contributing factor to this could be that the proportions of unknown compounds were higher at the higher temperatures, and some compounds of these unknowns could potentially belong to the OxyARs. Unknowns in this study were assigned to peaks which had no compound matched to it from the NIST library. The high unknowns at higher temperatures may be due to large molecules cracking to smaller fragments which could not be matched. The proportion of acids noticeably reduced with increased temperature as was the case with wood, and the sugars showed an upward trend with temperature rise suggesting increased depolymerisation reactions of holocellulose (cellulose/hemicellulose) [57]. Aliphatics were detected in highest quantity at 450 °C (3.89%) but diminished with the rise in temperature to 1.31% (500 °C) and 0.45% (550 °C). Aromatics were detected only at 500 °C (0.70%) and 550 °C (0.83%) while no PAHs were detected in the seed pods.

Overall, the leaves showed the least quantity of COI when compared to the other samples, which could be linked to their structure. The composition of biomass components of leaves is not available for comparison; however, it is noted that leaves contain the highest ash content thus reducing their energy potential (Table 4). The highest proportions of NITs were observed in the leaves compared to the other samples; this is expected due to the characteristics of leaves as they contain N-containing compounds such as tryptamine and phenethylamine as reported by Dahms et al. [58] which upon decomposing would lead to NITs formation. The nitrogen content is also highest in leaves as seen in Table 4.

Aliphatics were in notably high proportions in the leaves, compared to the wood and seed pods. This may be due to the catalytic action of the ash constituent which promoted reactions which formed aliphatics. The highest proportion detected was at 500 °C (11.13%) and lowest at 550

°C (9.44%) suggesting that at higher temperature, aliphatics could have depleted due to contributed to the formation of other compounds through reactions such as aromatisation [50]. These were mainly long chain aliphatics ranging from C₁₆ – C₂₁ such as Heneicosane. Aromatics such as ethyl benzene and styrene were observed to be at higher quantities in the leaves than other samples, the quantity increases from (2.33%) (450 °C) to 3.49% observed at both 500 and 550 °C suggesting that the composition of leaves supports the production of aromatics.

Products from the mixture samples show the highest proportion of COI in the WOSDLV sample at 83.04% at 500 °C as seen in Figure 7. It could be because there were less unknowns in this test as more peaks were effectively assigned compounds, which was not the case for the wood sample as it had more unknowns. It may be concluded that if *P. juliflora* fractions were to be pyrolysed as a mixture, it would yield a significant quantity of products that could effectively be converted to aromatics. The proportions of sugar and acids reduced with the rise in temperature due to increased thermal cracking as was observed by [25, 26].

The SDLV mixture (Figure 8) had the highest proportions of aliphatics which could be contribution of leaves to the products. The COI were less compared to WOSDLV with highest amount observed at 550 °C (76.37%) followed by 450 °C (70.41%) and lastly 500 °C (64.17%). This suggests that it may be beneficial to mix all fractions of the plant as pyrolysis raw material as opposed to separating them which would simplify the harvesting and production process, thus aiding to save on production costs.

Table 6: Functional groups assigned to products of py-GC/MS

Functional group	Abbreviation
Acids	AC
Alcohols	AL
Aliphatics	ALI

Functional group	Abbreviation
Aldehydes	ALD
Aromatics	AR
Ethers	ETH
Esters	EST
Ketones	KET
Oxygenated aromatics	OxyAR
Phenols	PH
Polyaromatic hydrocarbons	PAHs
Nitrogenous compounds	NITs
Sugars	SUG
Unknown	UN

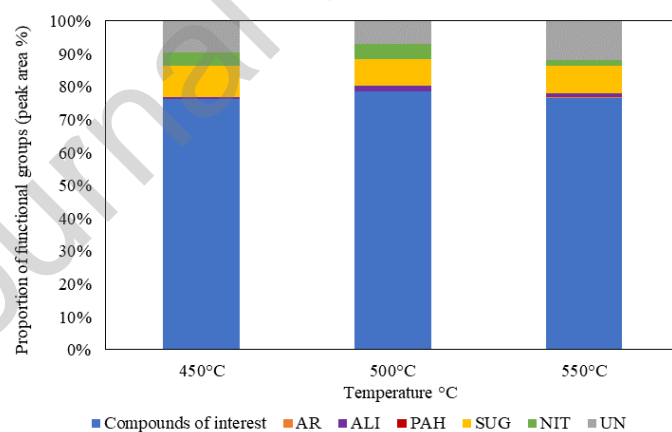


Figure 4: Products obtained from thermal pyrolysis of *P. juliflora* wood at 450, 500 and 550

°C.

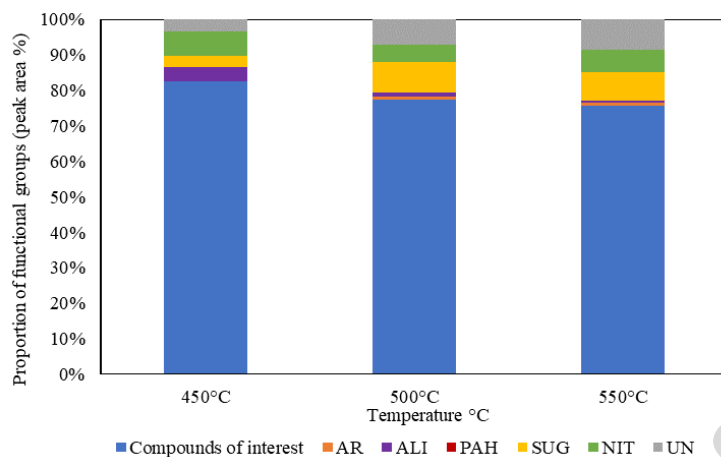


Figure 5: Products obtained from thermal pyrolysis of *P. juliflora* seed pods at 450, 500 and 550 °C.

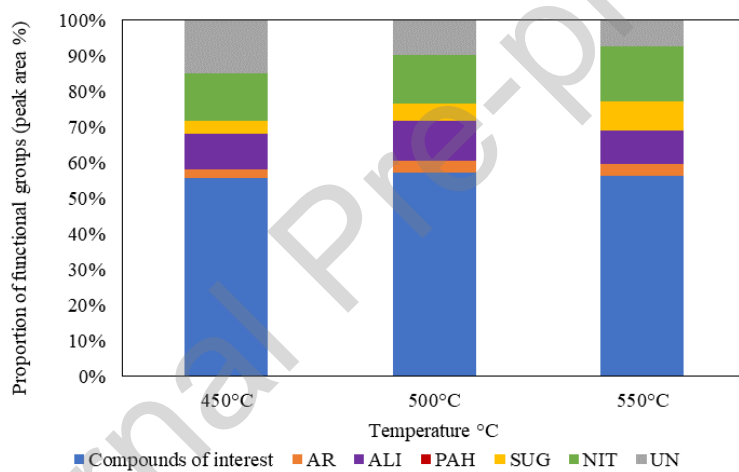


Figure 6: Products obtained from thermal pyrolysis of *P. juliflora* leaves at 450, 500 and 550 °C.

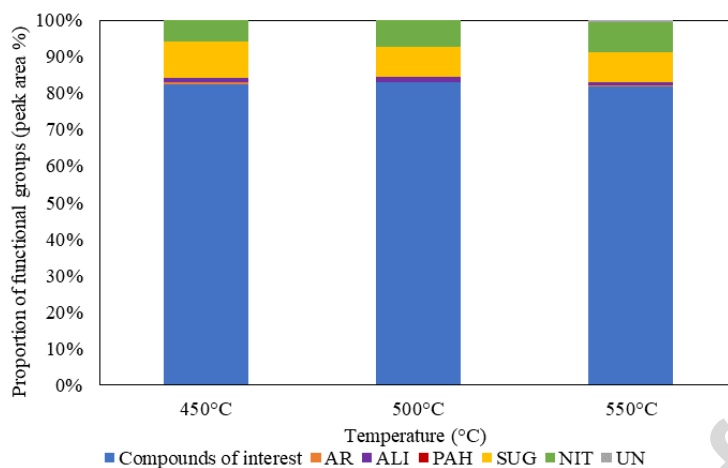


Figure 7: Products obtained from thermal pyrolysis of *P. juliflora* wood, seed pods, leaves mixture (80:10:10) at 450, 500 and 550 °C.

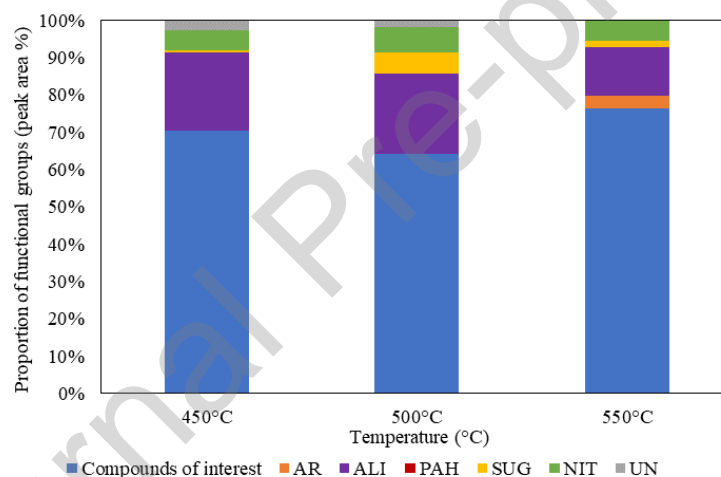


Figure 8: Products obtained from thermal pyrolysis of *P. juliflora* seed pods and leaves mixture (50:50) at 450, 500 and 550 °C.

4.3.2 Catalytic pyrolysis

The products obtained from performing catalytic py-GCMS of *P. juliflora* wood at 500 °C and C/B ratios of 3:1, 6:1 and 9:1, were studied for the formation of aromatics from the upgrading reactions. This was the optimum temperature observed for products that can be converted to aromatics for application in transportation fuel i.e., compounds of interest (COI). Catalytic tests were conducted on the wood sample as it gave the highest yield of COI at 500 °C. The catalysts used were HZSM-5, 1wt% Ni-HZSM-5 and 5wt.% Ni-HZSM-5 to evaluate the performance

of each catalyst and the effect of metal loading in the production of aromatics at each condition. Figure 9 to 11 show the proportions of functional groups from the thermal and catalytic pyrolysis of *P. juliflora* wood. The chromatogram obtained from catalytic pyrolysis of *P. juliflora* wood at 500 °C with 5wt.% Ni-HZSM-5 is available in supplementary material (Figure S2). As observed in the previous section, compounds obtained from thermal pyrolysis of *P. juliflora* are predominantly oxygenates (acids, ketones, aldehydes, phenols, furans and sugars) which would lead to high acidity, low heating value and instability of bio-oil [7]. Zeolite catalyst activity over pyrolysis vapours promotes important reactions in upgrading including deoxygenation, decarboxylation, dehydration, cracking, oligomerization, alkylation, isomerization, cyclization, and aromatization over its acid sites [8, 22].

The catalyst characterisation data (Table 5, Figure 5) demonstrates the micropore and mesopore distribution in the catalysts would promote formation of aromatics [37]. PAHs were also detected which is in line with work reported about the performance of these catalysts [11, 20, 22, 48]. The highest C/B ratio (9:1) resulted in the highest proportion of aromatics for all the catalysts. 5wt% Ni-HZSM-5 gave the highest proportion of aromatics (60.28%) followed by 1wt.% Ni-HZSM-5 (56.50%) and lastly HZSM-5 yielded 53.90% indicating that addition of Ni improved aromatics formation. The addition of Ni is reported to cause transition metal-assisted hydrogenation of compounds to form aromatics [59]. This is consistent with the findings of Yung et al. [20] and Veses et al [21] who attributed this to the presence of strong Lewis sites at the surface of the zeolite. The increased S_{BET} and pore volume (Table 5) from the characterisation of the Ni-loaded catalysts improved the effectiveness of the catalyst in producing aromatics [60]. Yung et al. [20] also noted a decrease in oxygenates with the Ni loaded catalysts compared to the HZSM-5, this is contrary to the findings of this study as higher proportions of oxygenates were obtained when Ni was present, which could be linked to the presence of Ni species on the catalyst surface which affected activity of acid sites on the zeolite

supports. They however noted that there was no noticeable trend with the increase of Ni loading with regards to the reduction of oxygenates [20]. Comparing the C/B ratio in all the catalysts, the least quantity of oxygenated compounds was found in HZSM-5. In the case of PAHs, less proportions were detected in the Ni loaded zeolites than in non-metal loaded as indicative in Figure 10 and 11 showing selectivity was towards aromatics. This would be preferred as it would prevent coke formation from PAHs' inability to go through the catalyst pores due to their size, which ultimately blocks catalyst pores and causes deactivation [27].

An increase in catalyst loading across all tests enhanced performance in terms of deoxygenation reactions and formation of aromatics which is due to high availability of acid sites with the increased quantity of catalyst [22, 46]. The aromatics included benzene and its derivatives such 1-ethylene-2-methylbenzene, also toluene, xylenes, styrene and Indane/Indene and its derivatives (2,3-dihydro-5-methyl-1H-Indene). The PAHs detected were naphthalene and its derivatives like 1-methylnaphalene and 2,6-dimethylnaphthene, phenanthrenes (phenanthrene, 3-methylphenanthrene and 2,7-dimethylphenanthrene), and Flourenes (flourene and 1-methyl-9H-flourene). Oxygenates were mostly furanic compounds which can be linked to their formation as intermediates from the decomposition reactions of holocellulose and lignin which lead to aromatic formation under further catalytic activity [17, 46]. The reduction of these furanic compounds with increased C/B ratios show greater catalyst presence enhanced their contribution to formation of aromatics [17, 46]. The compounds detected in this study have been reported in upgraded pyrolysis vapours using HZSM-5 [17, 20-22, 46, 48, 52]. Some NITs were detected in all the catalytic tests, these were mainly amides, it was observed that they decreased in proportion as the C/B ratio increased because of increased catalyst dose and thus enhanced catalytic activity. The reduction of NITs in bio-oil has also been observed by Maisano et al. [53] and Campanella & Harold [61] who reported the denitrogenation of bio-oil in the

presence of zeolite catalysts. The significant reduction in acid proportions across all tests shows the action of the zeolites in decomposing the acids to form smaller molecules [46].

The use of zeolites has proven to improve the product distribution of pyrolysis vapours from the pyrolysis of *P. juliflora*. This is due to the significant reduction in the proportion of acids and other oxygenates which are the causes of the limitations of bio-oil as it is corrosive, highly viscous, has low stability and heating value. The catalysts promote the production of aromatics such as benzene, toluene and xylene which are desired compounds in transportation fuel. The Ni-loaded resulted in higher proportions of monocyclic aromatics than PAHs which is what would be preferred as it would result in less coke formation due to less proportion of large molecules of PAHs which promote coke deposition as they block catalyst pores due to their size [27]. As there would be reduced PAHs formation, there would be less coke formation, resulting in longer catalytic activity and thus better performance as there will be low deactivation [27].

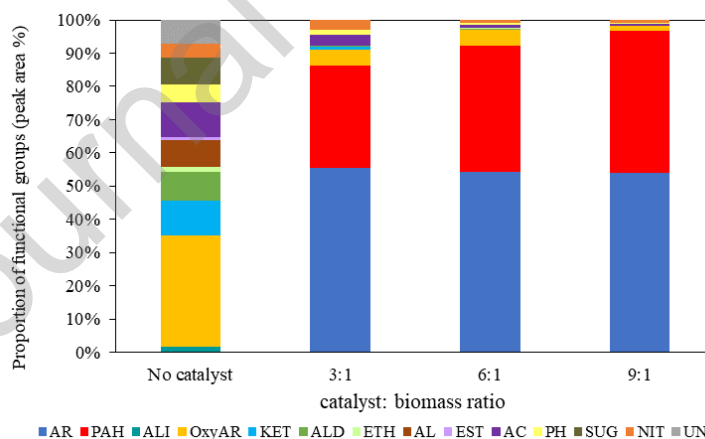


Figure 9: Products obtained from catalytic pyrolysis of *P. juliflora* wood at three catalyst:biomass ratios at 500 °C with HZSM-5.

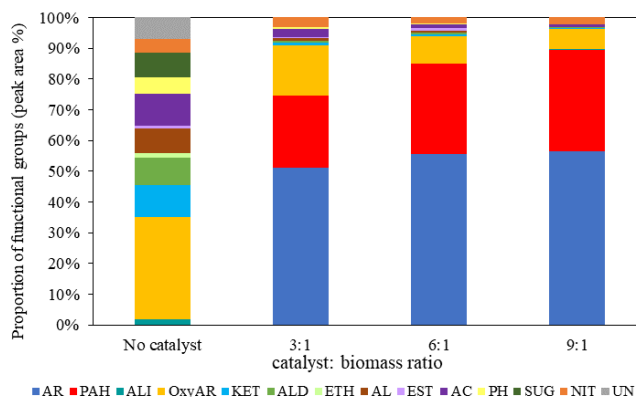


Figure 10: Products obtained from catalytic pyrolysis of *P. juliflora* wood at three catalyst: biomass ratios at 500 °C with 1wt.% Ni-HZSM-5.

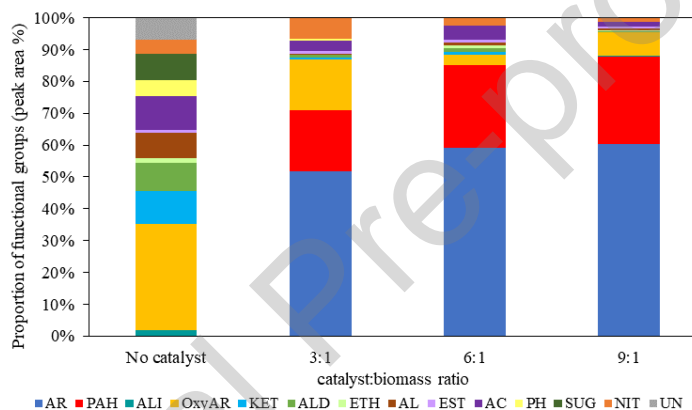


Figure 11: Products obtained from catalytic pyrolysis of *P. juliflora* wood at three catalyst: biomass ratios at 500 °C with 5wt.% Ni-HZSM-5.

5. Conclusions

This work provides an insight on the characteristics of three *P. juliflora* fractions, wood, seed pods, leaves, and their mixtures (WOSDLV; SDLV); and studies the pyrolysis product distribution from thermal and catalytic tests (using zeolite and zeolite-nickel catalysts). To date, there has been no previous work reporting the composition of the leaves and mixtures. Thermal py-GC/MS tests were conducted on these samples at 450, 500 and 550 °C; whereas catalytic tests were conducted on the wood sample at 500°C in the presence of HZSM-5, 1wt.% Ni-HZSM-5 and 5wt.% Ni-HZSM-5 at catalyst: biomass (C/B) ratios of 3:1, 6:1 and 9:1. The following conclusions were drawn:

1. A high proportion of compounds of interest (COI: 83.04%) were obtained from the wood, seed pods and leaves mixture (WOSDLV) at 500 °C.
2. Considerable percentages of acids, sugars, oxygenates, and nitrogenous compounds (NITs) were detected in the thermal tests, suggesting pyrolysis vapours need to be upgraded.
3. The catalytic tests showed a remarkable reduction in oxygenates, NITs and acids, whilst producing significant amounts of aromatics (i.e., benzene, toluene, xylenes) and PAHs (i.e., naphthalene, fluorene, and their derivatives). Aromatic production is important due to their application in transportation fuels.
4. Aromatics and PAHs yields were greater at a higher catalyst loading (C/B = 9:1) for all catalysts; whilst the addition of nickel resulted in higher selectivity towards aromatics by increasing its yield and reducing PAHs. The highest proportion of aromatics (60.28%) was attained using the 5wt.% Ni-HZSM-5, which also reduced acids and oxygenates.
5. *P. juliflora* is a viable candidate for biofuel production, and therefore these invasive species can be utilized for bioenergy, whilst their spread is being managed. These results can propose alternatives for regions around the world dealing with this invasive species.

Acknowledgements

This PhD research project is supported by the Botswana International University of Science and Technology through providing a full scholarship to the first author. The authors would like to thank the Clean Energy Building, Huazhong University of Science and Technology (HUST) for access to their analytical equipment for catalyst characterisation, as well as the EU Horizon 2020 Research and Innovation Program under the Marie Skłodowska-Curie Action (Grant Agreement No. 823745) for funding the secondment undertaken at HUST.

6. References

1. Pasiiecznik, N. M., P. J. C. Harris, and S.J. Smith, *Identifying Tropical Prosopis Species: A field guide*. 2004, Coventry, United Kingdom: HDRA Publishing.
2. Schachtschneider, K. and E.C. February, *Impact of Prosopis invasion on a keystone tree species in the Kalahari Desert*. *Plant Ecology*, 2013. **214**: p. 597-605.
3. Mosweu, S., C.M., Tibangayuka Kabanda, Mofatt Setshogo, Mbaki Muzila *Prosopis L. Invasion in the South-Western Region of Botswana: The Perceptions of Rural Communities and Management Options*. *Natural Resources*, 2013. **4**: p. 496 - 505.
4. Kashe, K., et al., *Potential Impact of Alien Invasive Plant Species on Ecosystem Services in Botswana: A Review on Prosopisjuliflora and Salvinia molesta*, in *Sustainability in Developing Countries*, Keitumetse S.O., Hens L., and N. D., Editors. 2020, Springer, Cham.
5. Animal Plant Health Agency, United Kingdom Government. *Invasive non-native (alien) plant species: rules in England and Wales*. 2023 [cited 2023 09/09/2023]; Available from: <https://www.gov.uk/guidance/invasive-non-native-alien-plant-species-rules-in-england-and-wales>.
6. Mukundan, S., G. Sriganesh, and P. Kumar, *Upgrading Prosopis juliflora to biofuels via a two-step pyrolysis – Catalytic hydrodeoxygenation approach*. *Fuel*, 2020. **267**(117320): p. 1 - 9.
7. Dhyani, V. and T. Bhaskar, *A comprehensive review on the pyrolysis of lignocellulosic biomass*. *Renewable Energy*, 2018. **129**: p. 695-716.
8. G. Kabir and B.H. Hameed, *Recent progress on catalytic pyrolysis of lignocellulosic biomass to high-grade bio-oil and bio-chemicals*. *Renewable and Sustainable Energy Reviews*, 2017. **70**: p. 945 - 967.

9. Bridgwater, T., *Challenges and Opportunities in Fast Pyrolysis of Biomass: Part II*. Johnson Matthey Technology Review, 2018. **62**(2): p. 150-160.
10. Wang, G., et al., *A Review of Recent Advances in Biomass Pyrolysis*. Energy & Fuels, 2020. **34**(12): p. 15557-15578.
11. Liang, J., G. Shan, and Y. Sun, *Catalytic fast pyrolysis of lignocellulosic biomass: Critical role of zeolite catalysts*. Renewable and Sustainable Energy Reviews, 2021. **139**: p. 110707.
12. Zhang, B., et al., *Catalytic fast co-pyrolysis of biomass and fusel alcohol to enhance aromatic hydrocarbon production over ZSM-5 catalyst in a fluidized bed reactor*. Journal of Analytical and Applied Pyrolysis, 2018. **133**: p. 147-153.
13. Hoff, T.C., et al., *Tailoring ZSM-5 Zeolites for the Fast Pyrolysis of Biomass to Aromatic Hydrocarbons*. ChemSusChem, 2016. **9**(12): p. 1473-1482.
14. Hu, X. and M. Gholizadeh, *Biomass pyrolysis: A review of the process development and challenges from initial researches up to the commercialisation stage*. Journal of Energy Chemistry, 2019. **39**: p. 109-143.
15. Bhoi, P.R., et al., *Recent advances on catalysts for improving hydrocarbon compounds in bio-oil of biomass catalytic pyrolysis*. Renewable and Sustainable Energy Reviews, 2020. **121**: p. 109676.
16. Thangalazhy-Gopakumar, S., et al., *Catalytic pyrolysis of green algae for hydrocarbon production using H⁺ZSM-5 catalyst*. Bioresource Technology, 2012. **118**: p. 150-157.
17. Zhang, M., F.L.P. Resende, and A. Moutsoglou, *Catalytic fast pyrolysis of aspen lignin via Py-GC/MS*. Fuel, 2014. **116**: p. 358-369.
18. Ding, K., et al., *Improving hydrocarbon yield from catalytic fast co-pyrolysis of hemicellulose and plastic in the dual-catalyst bed of CaO and HZSM-5*. Bioresource Technology, 2018. **261**: p. 86-92.

19. Iisa, K., et al., *In Situ and ex Situ Catalytic Pyrolysis of Pine in a Bench-Scale Fluidized Bed Reactor System*. Energy & Fuels, 2016. **30**(3): p. 2144-2157.
20. Yung, M.M., et al., *Biomass Catalytic Pyrolysis on Ni/ZSM-5: Effects of Nickel Pretreatment and Loading*. Energy & Fuels, 2016. **30**(7): p. 5259-5268.
21. Veses, A., et al., *Catalytic upgrading of biomass derived pyrolysis vapors over metal-loaded ZSM-5 zeolites: Effect of different metal cations on the bio-oil final properties*. Microporous and Mesoporous Materials, 2015. **209**: p. 189-196.
22. Lappas, A.A., et al., *Catalytic pyrolysis of biomass for transportation fuels*. WIREs Energy and Environment, 2012. **1**(3): p. 285-297.
23. Cai, R., et al., *Biomass Catalytic Pyrolysis over Zeolite Catalysts with an Emphasis on Porosity and Acidity: A State-of-the-Art Review*. Energy & Fuels, 2020. **34**(10): p. 11771-11790.
24. French, R. and S. Czernik, *Catalytic pyrolysis of biomass for biofuels production*. Fuel Processing Technology, 2010. **91**(1): p. 25-32.
25. Xin, X., et al., *The effect of biomass pretreatment on catalytic pyrolysis products of pine wood by Py-GC/MS and principal component analysis*. Journal of Analytical and Applied Pyrolysis, 2019. **138**: p. 145-153.
26. Bensidhom, G., et al., *Fast pyrolysis of date palm biomass using Py-GCMS*. Journal of the Energy Institute, 2021. **99**: p. 229-239.
27. Liu, Q., et al., *Promotion of monocyclic aromatics by catalytic fast pyrolysis of biomass with modified HZSM-5*. Journal of Analytical and Applied Pyrolysis, 2021. **153**: p. 104964.
28. Chandrasekaran, A., S. Ramachandran, and S. Subbiah, *Modeling, experimental validation and optimization of Prosopis juliflora fuelwood pyrolysis in fixed-bed tubular reactor*. Bioresource Technology, 2018. **264**: p. 66-77.

29. Gayathri, G. and K.B. Uppuluri, *The comprehensive characterization of Prosopis juliflora pods as a potential bioenergy feedstock*. Scientific Reports, 2022. **12**(1): p. 18586.
30. Chandran, R., et al., *Characteristics of bio-oil from continuous fast pyrolysis of Prosopis juliflora*. Energy, 2020. **190**: p. 116387.
31. Mythili, R., P. Subramanian, and D. Uma, *Biofuel production from Prosopis juliflora in fluidized bed reactor*. Energy Sources, Part A: Recovery, Utilization, and Environmental Effects, 2017. **39**(8): p. 741-746.
32. Carneiro-Junior, J.A., et al., *Valorization of Prosopis juliflora Woody Biomass in Northeast Brazilian through Dry Torrefaction*. Energies, 2021. **14**(12).
33. Yang, H., et al., *In-Depth Investigation of Biomass Pyrolysis Based on Three Major Components: Hemicellulose, Cellulose and Lignin*. Energy & Fuels, 2006. **20**(1): p. 388-393.
34. Pattiya, A., *1 - Fast pyrolysis*, in *Direct Thermochemical Liquefaction for Energy Applications*, L. Rosendahl, Editor. 2018, Woodhead Publishing. p. 3-28.
35. Suriapparao, D.V., N. Pradeep, and R. Vinu, *Bio-Oil Production from Prosopis juliflora via Microwave Pyrolysis*. Energy & Fuels, 2015. **29**(4): p. 2571-2581.
36. Ramos, R., et al., *Enhanced Production of Aromatic Hydrocarbons by Rapeseed Oil Conversion over Ga and Zn Modified ZSM-5 Catalysts*. Industrial & Engineering Chemistry Research, 2016. **55**(50): p. 12723-12732.
37. Fang, S., et al., *Influence of metal (Fe/Zn) modified ZSM-5 catalysts on product characteristics based on the bench-scale pyrolysis and Py-GC/MS of biomass*. International Journal of Energy Research, 2020. **44**(7): p. 5455-5467.

38. Zhou, W., et al., *4,6-Dimethyldibenzothiophene Hydrodesulfurization on Nickel-Modified USY-Supported NiMoS Catalysts: Effects of Modification Method*. Energy & Fuels, 2017. **31**(7): p. 7445-7455.
39. Li, J.-W., et al., *Effect of nickel on phosphorus modified HZSM-5 in catalytic cracking of butene and pentene*. Fuel Processing Technology, 2017. **159**: p. 31-37.
40. Barton, R.R., et al., *Ni/HZSM-5 catalyst preparation by deposition-precipitation. Part 1. Effect of nickel loading and preparation conditions on catalyst properties*. Applied Catalysis A: General, 2017. **540**: p. 7-20.
41. Hakimian, H., et al., *Production of valuable chemicals through the catalytic pyrolysis of harmful oil sludge over metal-loaded HZSM-5 catalysts*. Environmental Research, 2022. **214**: p. 113911.
42. Li, Z., et al., *Catalytic fast pyrolysis of rice husk over hierarchical micro-mesoporous composite molecular sieve: Analytical Py-GC/MS study*. Journal of Analytical and Applied Pyrolysis, 2019. **138**: p. 103-113.
43. ALothman, Z.A., *A Review: Fundamental Aspects of Silicate Mesoporous Materials*. Materials (Basel), 2012. **5**(12): p. 2874-902.
44. Wei, Q., et al., *Synthesis of Ni-Modified ZSM-5 Zeolites and Their Catalytic Performance in n-Octane Hydroconversion*. Frontiers in Chemistry, 2020. **8**.
45. Valencia, D. and T. Klimova, *Citric acid loading for MoS₂-based catalysts supported on SBA-15. New catalytic materials with high hydrogenolysis ability in hydrodesulfurization*. Applied Catalysis B: Environmental, 2013. **129**: p. 137-145.
46. Arabiourrutia, M., et al., *Catalytic pyrolysis of date palm seeds on HZSM-5 and dolomite in a pyroprobe reactor in line with GC/MS*. Biomass Conversion and Biorefinery, 2022.

47. Murillo, J.D., E.A. Ware, and J.J. Biernacki, *Characterization of milling effects on the physical and chemical nature of herbaceous biomass with comparison of fast pyrolysis product distributions using Py-GC/MS*. *Journal of Analytical and Applied Pyrolysis*, 2014. **108**: p. 234-247.
48. Carlson, T.R., et al., *Production of green aromatics and olefins by catalytic fast pyrolysis of wood sawdust*. *Energy & Environmental Science*, 2011. **4**(1): p. 145-161.
49. Asadieraghi, M., W.M.A. Wan Daud, and H.F. Abbas, *Model compound approach to design process and select catalysts for in-situ bio-oil upgrading*. *Renewable and Sustainable Energy Reviews*, 2014. **36**: p. 286-303.
50. Huber, G.W., S. Iborra, and A. Corma, *Synthesis of Transportation Fuels from Biomass: Chemistry, Catalysts, and Engineering*. *Chemical Reviews*, 2006. **106**(9): p. 4044-4098.
51. Leng, L., et al., *A review on pyrolysis of protein-rich biomass: Nitrogen transformation*. *Bioresource Technology*, 2020. **315**: p. 123801.
52. Kaewpengkrow, P.R., D. Atong, and V. Sricharoenchaikul, *Bio-fuel production from catalytic fast pyrolysis of Jatropha wastes using pyroprobe GC/MS and drop tube pyrolyzer*. *Journal of Analytical and Applied Pyrolysis*, 2022. **165**: p. 105574.
53. Maisano, S., et al., *Catalytic pyrolysis of Mediterranean sea plant for bio-oil production*. *International Journal of Hydrogen Energy*, 2017. **42**(46): p. 28082-28092.
54. Valencia, L., et al., *Nanolignocellulose Extracted from Environmentally Undesired Prosopis juliflora*. *ACS Omega*, 2019. **4**(2): p. 4330-4338.
55. Cheng, S., et al., *Effects of Ca and Na acetates on nitrogen transformation during sewage sludge pyrolysis*. *Proceedings of the Combustion Institute*, 2019. **37**(3): p. 2715-2722.

56. Zhan, H., et al., *Insights into the evolution of fuel-N to NO_x precursors during pyrolysis of N-rich nonlignocellulosic biomass*. *Applied Energy*, 2018. **219**: p. 20-33.
57. Dhyani, V. and T. Bhaskar, *Chapter 9 - Pyrolysis of Biomass*, in *Biofuels: Alternative Feedstocks and Conversion Processes for the Production of Liquid and Gaseous Biofuels (Second Edition)*, A. Pandey, et al., Editors. 2019, Academic Press. p. 217-244.
58. Dahms, H.-U., P. Malliga, and P. Sethuraman, *Pharmacological potentials of phenolic compounds from Prosopis spp.-a review*. *Journal of Coastal Life Medicine*, 2015. **2**.
59. Iliopoulou, E.F., et al., *Catalytic upgrading of biomass pyrolysis vapors using transition metal-modified ZSM-5 zeolite*. *Applied Catalysis B: Environmental*, 2012. **127**: p. 281-290.
60. Dai, L., et al., *Catalytic fast pyrolysis of torrefied corn cob to aromatic hydrocarbons over Ni-modified hierarchical ZSM-5 catalyst*. *Bioresource Technology*, 2019. **272**: p. 407-414.
61. Campanella, A. and M.P. Harold, *Fast pyrolysis of microalgae in a falling solids reactor: Effects of process variables and zeolite catalysts*. *Biomass and Bioenergy*, 2012. **46**: p. 218-232.

CRedit authorship contribution statement

Mpho Thabang Rapoo: Conceptualization; Data curation; Formal analysis; Funding acquisition; Investigation; Methodology; Resources; Validation; Visualization; Writing - original draft; and Writing - review & editing.

Saranpreet Singh: Data curation; Formal analysis.

Katie Chong: Conceptualization; Validation; Supervision; Writing - review & editing.

Scott Banks: Conceptualization; Validation; Supervision; Writing - review & editing.

Paula Blanco Sanchez: Conceptualization; Funding acquisition; Resources; Supervision; Validation; Visualization; Writing - review & editing.

Declaration of interests

The authors declare that they have no known competing financial interests or personal relationships that could have appeared to influence the work reported in this paper.

The authors declare the following financial interests/personal relationships which may be considered as potential competing interests:

Highlights

- *Prosopis* invasive plant can be converted to aromatics (biodiesel precursors).
- Fast pyrolysis of *Prosopis* leaves, seeds, wood, and their mixtures was evaluated.
- Ash and fixed carbon considerably varied in *Prosopis* individual fractions.
- Thermal and catalytic fast pyrolysis (CFP) of *Prosopis* can yield aromatics.
- CFP of *Prosopis* wood and 5wt% Ni-HZSM-5 catalyst yielded 60.3% of aromatics.